Current Biology 20, 2046–2051, November 23, 2010 ©2010 Elsevier Ltd All rights reserved DOI 10.1016/j.cub.2010.10.030

Report

Actomyosin Tube Formation in Polar Body Cytokinesis Requires Anillin in *C. elegans*

Jonas F. Dorn,[1] Li Zhang,[1] Véronique Paradis,[1] Daniel Edoh-Bedi,[1] Sylvester Jusu,[1] Paul S. Maddox,[1] and Amy Shaub Maddox[1,*]

[1]Institute for Research in Immunology and Cancer and Department of Pathology and Cell Biology, Université de Montréal, P.O. Box 6128, Station Centre-Ville, Montréal QC, H3C 3J7, Canada

Summary

Polar body extrusion (PBE) is the specialized asymmetric division by which oocytes accomplish reduction in ploidy and retention of cytoplasm. During maternal gametogenesis, as in male meiosis and mitosis, cytokinesis is accomplished by a ring rich in active Rho, myosin, and formin-nucleated F-actin [1–7]. However, unlike mitosis, wherein the contractile ring encircles the cell equator, the polar body ring assembles as a discoid cortical washer. Here we show that in *Caenorhabditis elegans*, the meiotic contractile ring transforms during closure from a disc above the spindle to a cylinder around the spindle midzone. The meiotic midbody tube comprises stacked cytoskeletal rings. This topological transition suggests a novel mechanism for constriction of an initially discoid cytokinetic ring. Analysis of mouse PBE indicates that midbody tube formation is a conserved process. Depletion of the scaffold protein anillin (ANI-1) from *C. elegans* results in large and unstable polar bodies that often fuse with the oocyte. Anillin is dispensable for contractile ring assembly, initiation, and closure but is required for the meiotic contractile ring to transform from a disc into a tube. We propose that cytoskeletal bundling by anillin promotes formation of the midbody tube, which ensures the fidelity of PBE.

Results

Like mitosis, maternal meiotic division requires microtubule-dependent chromosome segregation and actomyosin-based contractile ring closure, but the extreme asymmetry of maternal meiosis further requires eccentric anchoring of the spindle to the cell cortex. In mammals, amphibians, and echinoderms, perturbations of Rho or F-actin cause dissociation of the spindle from the cortex (reviewed in [8]), largely precluding the study of subsequent meiotic cytokinesis. In *Caenorhabditis elegans*, spindle migration and anchoring require microtubules, not F-actin [9]. Therefore, *C. elegans* is uniquely suited to explore actin-based molecular mechanisms of meiotic cytokinesis.

Anillin Is Required for the Fidelity of Polar Body Extrusion

Anillin is a scaffolding protein required for mitotic and spermatogenic cytokinesis across phylogeny (reviewed in [10]). Despite the biochemical and cell biological evidence that anillin organizes the contractile ring [11–20], the mechanical basis for cytokinesis failure following anillin depletion is poorly understood [13, 16, 18–22]. Only the terminal phenotype of failure has been reported for maternal meiotic cytokinesis [21, 23]. To understand how anillin contributes to this process, we performed differential interference contrast (DIC) time-lapse imaging of isolated, recently fertilized *C. elegans* embryos undergoing the final stages of maternal meiosis. In control embryos, first polar bodies formed soon after anaphase onset (Figure 1A). Polar bodies resulting from the first and second meioses were of characteristic size, which did not vary over the time of observation, indicating effective cytokinesis (Figure 1B). In anillin-depleted embryos, first polar bodies emerged normally after anaphase onset but grew larger than those in control cells and were unstable in size (Figures 1A and 1B, pink; see also Movie S1 available online). In approximately 25% of anillin-depleted cases (Figure S1A, orange), the first polar body released its contents back into the oocyte (Figure 1A). Second polar bodies tended to be larger than the first polar body, and they often failed to fully and permanently extrude (Figure 1B; Figure S1A). Although phenotypes varied, each of the 22 polar body extrusion events observed in anillin-depleted embryos was abnormal (Figure S1A).

To assess whether larger polar body size in anillin-depleted embryos corresponded to inappropriate inclusion of cytoplasm in the polar body, we compared the fluorescence intensity of soluble GFP-tagged myosin in polar bodies to that in the embryo proper using live-cell confocal imaging. Control polar bodies had lower soluble myosin fluorescence intensity than the embryo, indicating that they normally contain almost exclusively chromatin. By contrast, following anillin depletion, polar bodies contained soluble GFP-myosin comparable to that in oocyte cytoplasm (Figure S1B). These results demonstrate that anillin limits polar body size and suggest that, in this way, it contributes to the generation of oocytes competent for fertilization and development.

Because polar body extrusion failure could also occur after completion of meiosis, the results from time-lapse imaging (Figure S1A) likely underestimate the severity of the effects of anillin depletion. Indeed, when meiotic success was assessed somewhat later (by the presence of excess chromatin during the first zygotic mitosis), 77% of anillin-depleted embryos were grossly aneuploid (Figure 1D). Thus, the role of anillin in maintaining polar body size and stability likely accounts for a large proportion of the 100% embryonic lethality seen following anillin depletion [21].

The Meiotic Contractile Ring Transforms from a Disc into a Tube

Anillins throughout phylogeny are required for cytoskeletal organization during cytokinesis [10]. To understand anillin's role in the contractile mechanism of polar body cytokinesis, we first examined the meiotic contractile ring in control cells by imaging embryos expressing GFP-tagged myosin (NMY-2:GFP) and mCherry-tagged histone to follow chromosomes and cell-cycle progression. In control cells, the chromosomes (and thus spindle) localized to the embryo cortex in a region free of myosin (Figure 2A; Movie S1). Therefore, a rough ring of myosin crowned the spindle before anaphase. Upon

*Correspondence: amy.maddox@umontreal.ca

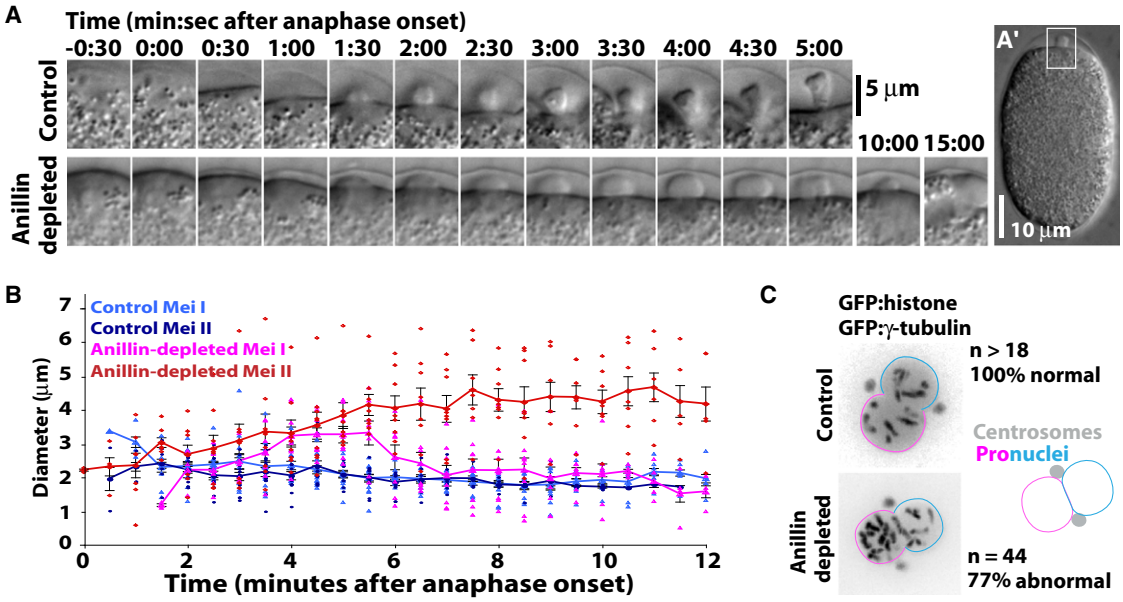

Figure 1. Anillin Is Required for the Small and Constant Size, and Successful Extrusion, of Polar Bodies

(A) Still images from DIC time-lapse imaging show cortical dynamics during polar body extrusion (PBE). Anaphase onset was determined using the mCherry:histone signal from simultaneous fluorescence imaging of the same cells.

(A′) DIC image of entire control embryo showing region cropped for (A).

(B) The smallest diameter of each polar body is plotted over time (lines denote averages; bars represent standard error of the mean [SEM]).

(C) Gross embryonic aneuploidy (abnormal) was noted by the presence of supernumerary chromosomes in the maternally derived (pink) pronucleus, as judged from full Z series imaging of GFP-tagged histone or DAPI (not shown).

anaphase onset, the myosin patches surrounding the spindle coalesced into a coherent discoid ring, or washer shape. As the ring constricted, it became centered between the segregated masses of chromatin and closed around the spindle midzone (see Figure 3A).

The contractile ring underwent a topological transition as it closed, from a two-dimensional washer to a three-dimensional tube. This transformation occurred concomitant with closure (Figures 2A and 2D). As a result, the meiotic cytokinetic ring acquires a large area of contact with the spindle midbody (see Figure 3A), similar to the conformation of mitotic midbodies [24]. Furthermore, myosin, F-actin, and anillin colocalize in meiotic midbody long after closure (Figures 2A, 2E, and 2F; Figure 3A; Figures S2A and S2B). The transformation from discoid washer to tube also occurs when polar body extrusion takes place in the worm uterus (Figure S2C; see also Figure 3), and it is therefore not a result of stresses on dissected newly fertilized embryos.

The Meiotic Midbody Comprises a Stack of Rings

We next explored the mechanical basis of the shape change of the meiotic contractile ring. We hypothesized that the combined effects of bundling and contraction within the F-actin and myosin cytoskeleton (referred to collectively as actomyosin) facilitated discoid-to-tube transformation. In support of this idea, F-actin in the meiotic contractile ring of the freshwater annelid worm *Tubifex* becomes progressively circumferentially bundled during constriction [25]. This would occur most efficiently at the inner edge of the washer, and, as a second ring formed and constricted, it would push the first minimal-diameter ring away from the oocyte cortex (toward the forming polar body), promoting extension of the tube (Figure 2C). A similar process could result in formation of a continuous coil. Either morphology is consistent with a transformation of the cytokinetic discoid washer that requires both cytoskeletal bundling and contractility. In support of this hypothesis, myosin appeared as paired dots on either side of a single confocal section of the midbody tube (Figure 2B; see also Figure 3E) and as rings in a 3D reconstruction (Movie S2). To confirm that fluorescently tagged myosin accurately reported dynamics of the actomyosin cytoskeleton, we visualized endogenous F-actin in meiotic embryos with fluorescent phalloidin. Early in anaphase, the spindle abutted the cortex in an F-actin-free patch (as for myosin; Figure 2A) and was thus surrounded by a planar F-actin-rich washer (Figure 3A). In late anaphase, the contractile ring appeared as a tube with extensive contact with the narrowing spindle midzone. Long after polar body extrusion, as the embryo underwent its first mitotic division, F-actin remained visible in the meiotic midbody (Figure 3A).

To assess the presence of discrete circumferential actomyosin rings in meiotic midbodies, we analyzed single optical sections of embryos stained with phalloidin or expressing GFP-tagged myosin or anillin for the presence of multiple paired dots, which we reasoned would be evidence of stacked rings (Figure 3B, schematic). We quantified the presence of matched peaks of fluorescence on either side of the midbody tube by performing a line scan image analysis. Profiles generated by line scan were analyzed to determine correlation between peaks and valleys in fluorescence intensity (see Experimental Procedures). Comparing the two line scans for the sides of each midbody revealed that these structures are highly ordered, comparing favorably with the analysis of two line scans of skeletal muscle (Figure 3E; Figure S3). By contrast, when each midbody line scan was compared to another region of the embryo cortex, little correlation was detected (Figure 3C, gold line; Figure 3E). Paired peaks of phalloidin staining were also observed on the midbodies of

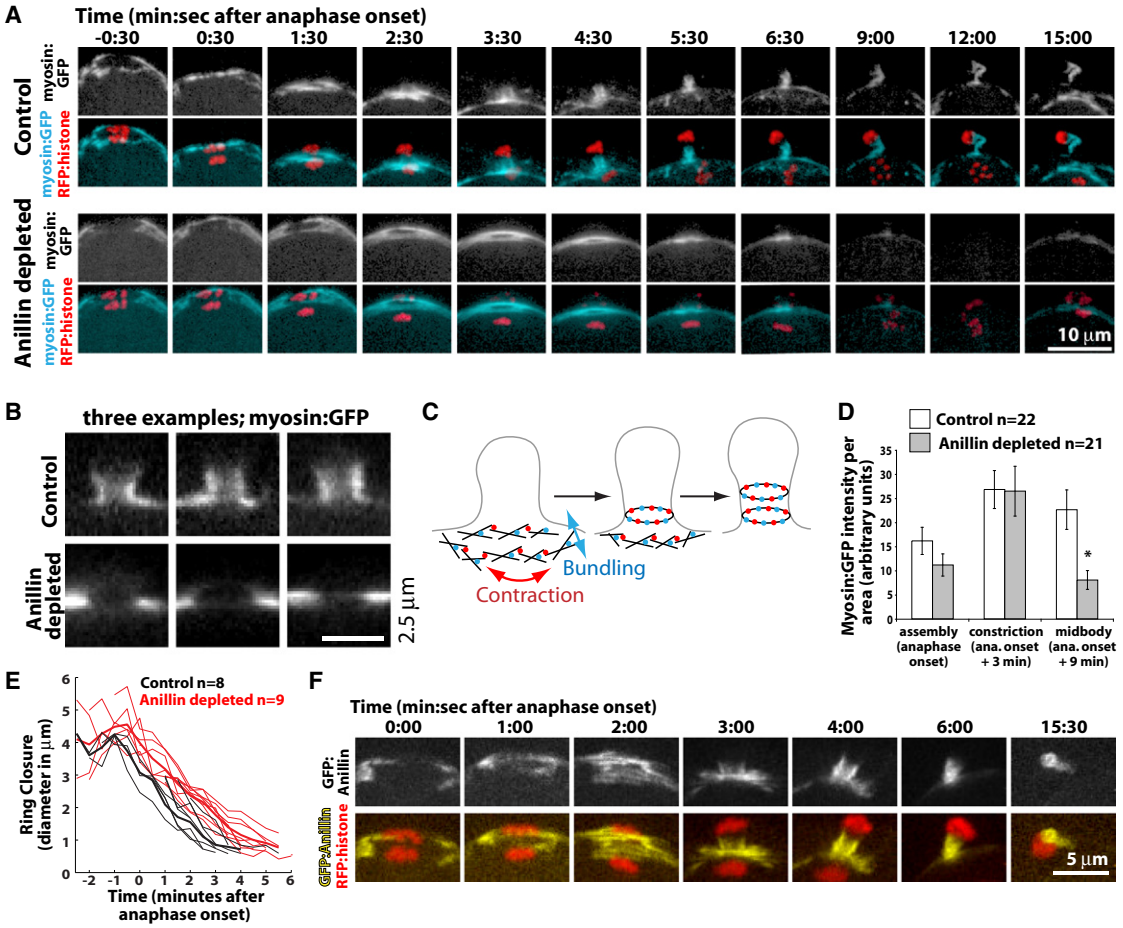

Figure 2. Anillin Is Required for the Polar Body Contractile Ring to Transform from a Disc to a Tube

(A) Still images from fluorescence time-lapse imaging of embryos expressing GFP-tagged myosin heavy chain (NMY-2; myosin:GFP) and mCherry-tagged histone (RFP:histone) show dynamics of the actomyosin cytoskeleton and chromatin during PBE. Images are maximum-intensity projections of nine 1 μm spaced confocal sections acquired for each time point. All images for both conditions were scaled identically.

(B) Single confocal sections through the middle of the contractile rings demonstrate the hollow center of the midbody tube. Examples from three different cells per condition are shown.

(C) Schematics illustrate hypothesis of the combined effects of bundlers (blue dots) and motors (red dots) on organization of the cytoskeleton (black lines).

(D) Myosin recruitment to and compaction within the contractile ring is not significantly ($p > 0.08$) affected by anillin depletion, but more myosin is lost following anillin depletion (*$p < 0.002$; error bars represent SEM).

(E) Kinetics of ring closure, measured as the inner diameter of the contractile ring from rotated Z series time-lapse sequences. Thin lines denote individual cells; thick lines denote averages.

(F) GFP-tagged anillin localizes to the contractile ring throughout closure and morphogenesis.

mouse oocytes (Figures 3E and 3F). Two to four rings comprised the stacks (*C. elegans* phalloidin: 2.5 ± 0.7, myosin: 2.2 ± 0.4, and anillin: 3.0 ± 1.0; mouse phalloidin: 2.9 ± 0.9 [mean ± standard deviation]). Together, our findings suggest that a stack of actomyosin rings, or a single actomyosin coil, forms during polar body cytokinesis.

Anillin Is Dispensable for Many Aspects of Meiotic Cytokinesis

Anillin is present in the meiotic contractile ring throughout assembly and closure and persists in the midbody tube (Figure 2F; [21]), suggesting that it could have essential roles at any stage of polar body cytokinesis. In anillin-depleted embryos, the spindle properly abutted the cortex at a zone poor in myosin and F-actin (Figure 2A; Figure 3A; Movie S1). The planar metaphase rings in anillin-depleted cells were slightly larger than those in controls but also contained slightly less myosin per area; thus, actomyosin recruitment during ring assembly appeared normal (Figures 2A, 2D, and 2E; [21]). After anaphase, cytokinesis commenced with normal timing, and the rate of ring constriction was not affected by anillin depletion (Figure 2E). Anillin depletion resulted in a slight delay in furrow completion (Figure 2E). However, this delay does not account for failure of polar body production: reentry of polar body DNA into the embryo usually (80%, n = 10) occurred via reopening of a connection with the oocyte after complete contractile ring closure. Together, these results demonstrate that many aspects of contractile ring function do not depend on anillin.

Anillin Is Required for the Topological Transition of the Meiotic Contractile Ring

Because anillin robustly bundles F-actin and binds myosin and the septins [11–13], we hypothesized that it drives the transformation of the cytokinetic ring from disc to tube via

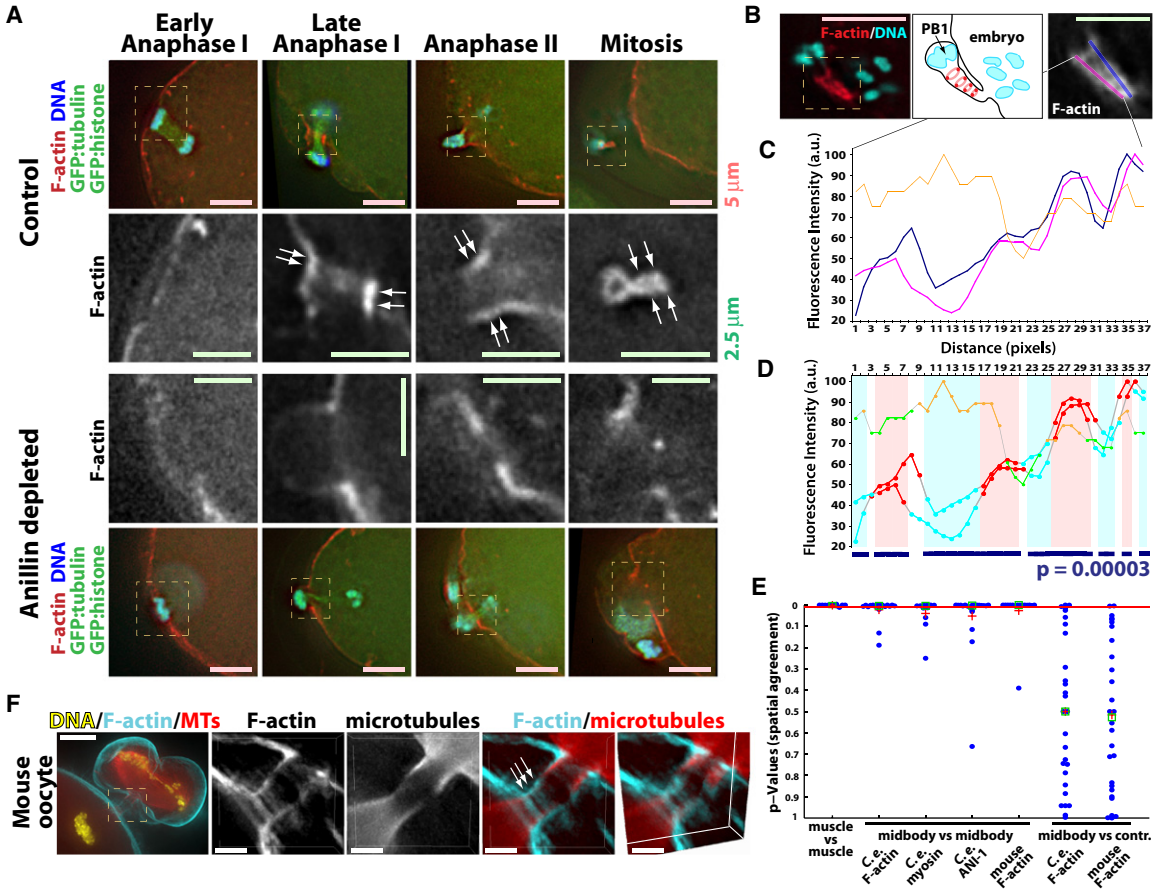

Figure 3. Anillin Is Required for Actin Rings in the Meiotic Midbody

(A) Single optical sections of embryos expressing GFP-tagged tubulin and histone and stained with phalloidin to label F-actin and with DAPI. Examples of approximately the same cell-cycle stage, as determined according to spindle and chromatin morphology, are shown for control embryos and those depleted of anillin. Phalloidin-staining-only panels are magnifications of yellow-dashed boxes in corresponding color overlays. Arrows denote paired dots of F-actin fluorescence.

(B) Example and schematic of line scans drawn along the sides of the midbody (single optical section). Scale bars represent 5 μm (pink) and 2.5 μm (green).

(C) Blue and purple line scans show phalloidin fluorescence intensity along the length of the midbody. Gold trace represents a negative control line scan of another part of the cortex.

(D) Each point on line scans was designated as part of a peak (red) or valley (cyan; or orange and green for negative control line scans), based on whether it was above or below the local average. Colored bars highlight points for which both lines had a peak or valley. Bar below graph illustrates proportion of points that were in agreement (both peak or valley) for the line scan; p value shown is the probability of observing the agreement between line scan pairs by random chance.

(E) Scatter plot of binomial test results. Muscle (see Figure S1D) served as a positive control. Comparison of half-ring scans with another region of the cortex served as negative controls. Red bar denotes 0.01; red cross denotes mean; green box denotes median.

(F) Maximum-intensity projections through 9 μm of a mouse oocyte stained with phalloidin, α-tubulin antibody, and DAPI. For magnified view, a rotated volume view is shown to reveal F-actin banding on the side of the midbody (visible as puncta in the orthogonal projection [arrows]). Scale bars represent 10 μm (first) and 2.5 μm (remaining).

directing cytoskeletal organization. Indeed, in anillin-depleted cells, the contractile ring remained a homogenous discoid washer that approached the spindle midzone in a single plane throughout meiotic anaphase (Figures 2A and 2B; Figure 3A; Movie S1). Interestingly, this demonstrates that the disc-to-tube transformation is not a physical inevitability of contraction, but rather requires anillin. We hypothesize that the stacked-rings conformation facilitated by anillin promotes the effective processivity of actomyosin contraction (myosin could more persistently encounter a filament track if F-actin and myosin are colinear; see Figure 4A). In support of this idea, F-actin, myosin, and anillin persist in the midbody long after closure in control cells (Figures 2A, 2D, and 2F; Figure 3A), but myosin is lost from the meiotic midbody following anillin depletion (Figures 2A and 2D). Taken together, our results indicate that anillin contributes to the success of polar body extrusion by organizing actomyosin into multiple stacked rings, thus generating a midbody tube with extensive contact with the midzone.

The many protein-protein (and potential protein-lipid) interactions of anillin engender myriad hypotheses to explain its mode of action. The tubular midbody may directly promote permanent scission of the polar body from the oocyte by creating a minute cytoplasmic bridge conducive to the membrane dynamics of abscission (Figure 4B). Anillin could contribute to meiotic cytokinesis by coupling the actomyosin cytoskeleton to midzone microtubules directly, or it could contribute to meiotic cytokinesis indirectly via association with the RhoGAP component of the centralspindlin midzone-binding complex, as has been seen for *Drosophila* anillin

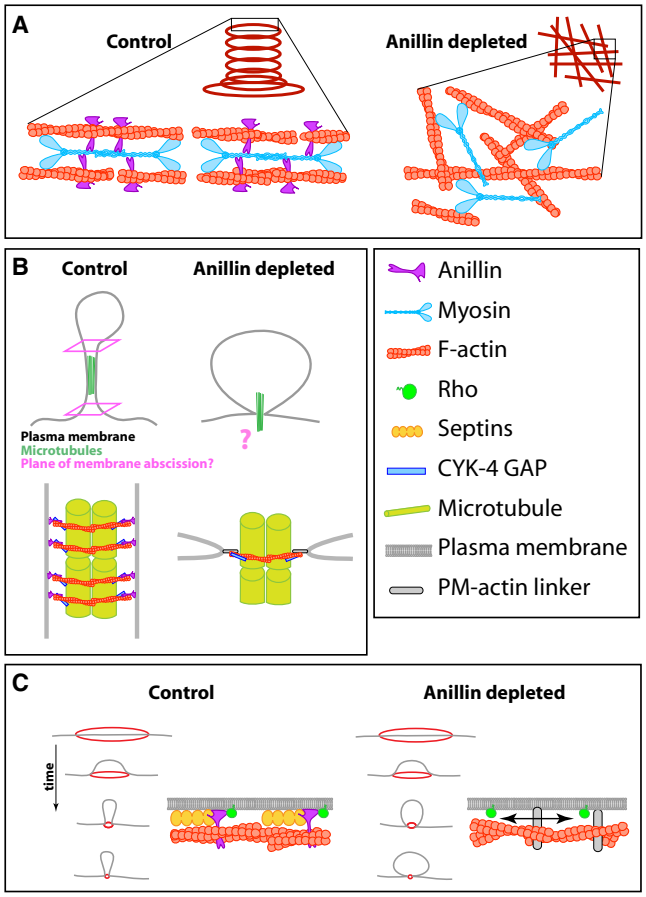

Figure 4. Schematic Summaries and Hypotheses for Anillin's Mode of Action

(A) Anillin promotes myosin processivity by aligning F-actin and myosin.

(B) Anillin promotes abscission by coupling actomyosin rings to the meiotic spindle midzone.

(C) Anillin limits polar body expansion by linking the actomyosin cytoskeleton to the plasma membrane. Double-headed arrow denotes increased mobility in the plane of the membrane following anillin depletion. Components are drawn to approximate scale, except in the key.

[14, 15, 17] (Figure 4B). Additionally, anillin may participate in a contractile ring-intrinsic mechanism for limiting polar body surface area, and thus volume, by restricting the mobility of the lipid bilayer past the ring (Figure 4C). Such a role could be mediated by interaction of anillin with the plasma membrane, either directly or via the septins [12, 18, 26]. Future work with anillin truncations lacking specific interaction domains, computational modeling, and in vitro studies will elucidate how this conserved protein ensures the fidelity of meiotic cytokinesis and how these roles contribute to contractile ring function in general.

Experimental Procedures

C. elegans Strains

Nematodes were maintained using standard procedures. See Table S1 for strain names and genotypes.

Live-Cell Imaging

Newly fertilized embryos undergoing maternal meiotic division were isolated and imaged approximately as by [27]. Briefly, gravid adults were placed on a coverslip in 4 μl meiosis medium (0.6× Leibowitz-15 media, 0.2× heat-inactivated fetal bovine serum, 25 mM HEPES pH 7.4, 5 mg/ml inulin), held with fine forceps, cut, and stripped of all embryos. The droplet was encircled by a 1 cm diameter ring of Vaseline and compressed so that the droplet and the Vaseline made contact with two coverslips. Embryos were not compressed. Embryos were imaged at 45× (using a Nikon PlanApo 60× oil objective, a 1.5× optivar, and 2 × 2 binning) on a Nikon TE-2000 inverted microscope equipped with an OrcaER camera, operated by MetaMorph software (Molecular Devices).

RNA-Mediated Interference

Because of the lack of a loss-of-function allele of *ani-1*, we removed anillin function by thorough (~95%) protein depletion via RNA interference as described [21].

Imaging Measurements

MetaMorph software was used for all measurements unless otherwise noted. For Figure 1B (polar body diameter), the shortest diameter of the polar body proper (excluding the neck) was measured. For Figure S1B (cytoplasmic intensity), the fluorescence intensity of soluble NMY-2:GFP within a region in the embryo was subtracted from the intensity in a region of the same size with the polar body. For Figure 2D (myosin intensity per area), maximum-intensity projections from time-lapse Z series were used to measure the intensity of myosin:GFP in an ~3 μm square region within the meiotic contractile ring, which was normalized by subtracting the intensity in a region of the same size outside the ring. For Figure 2E (ring closure rate), meiotic contractile ring inner diameter was measured from time-lapse Z series image data that was rotated and projected in the spindle axis using custom MATLAB-based software (cyanRing; available upon request). For Figures 3B–3D (ring detection), line scans were drawn along the meiotic midbody, as in the schematic, and intensity values were designated as part of a "peak" or a "valley" (above or below the local average [average of the local minimum and maximum]). Line scans were compared pixel by pixel: the number of pixels classified as peak or valley on both line scans was counted (Figure 3D, shading). The degree of agreement between pairs of line scans (both sides of the midbody or, for controls, one side of a midbody and one line scan taken from elsewhere on the embryo cortex) was calculated from the total number of points and the number for which the score (peak versus valley) was the same. The binomial distribution test (Microsoft Excel) was applied to determine the likelihood of obtaining a given number of equally classified pixels for each pair of midbody line scans, assuming that it was equally likely for two pixels to be classified as the same or different.

Fixed-Cell Staining

For *C. elegans*: slides were coated with 801 mM chromalum, 4 mg/ml gelatin, and 1 mg/ml poly-L lysine and dried overnight. Gravid hermaphrodites were dissected in a drop meiosis medium, which was then drawn off to bring embryos to the surface of the slide. A drop of fixative (60 mM PIPES pH 6.9, 10 mM EGTA, 25 mM HEPES, 1 mM $MgCl_2$, 4% electron microscopy-grade formaldehyde, 0.2% glutaraldehyde, 0.1 mg/ml lysolecithin [Sigma C-6137], 100 mM dextrose) was applied to the worm/embryo patch and incubated for 15 min at room temperature [28]. Slides were washed in three changes of phosphate-buffered saline (PBS) in coplin jars. Samples were incubated with 5 units/ml AlexaFluor 546 phalloidin (Molecular Probes) for 1 hr in the dark and then mounted under #1.5 coverslips in Vectashield (Vector Laboratories) with DAPI to stain chromatin. We were unable to find a condition that allowed preservation of F-actin and staining with antibodies in meiotic embryos, including when we added chitinase to the dissection medium to compromise the eggshell. Therefore, strains expressing GFP-tagged proteins were used (see Table S1 for strain information).

For mouse: oocytes were harvested from 6- to 11-week-old mice and placed in 37°C M16 medium + 4 mg/ml bovine serum albumin (BSA), 50 ug/ml dibutiryl cAMP (Sigma). After 2 hr, oocytes were washed into M2 + BSA, and the zona pellucida was removed with Tyrode's acid. Oocytes were allowed to undergo maturation in M16 + BSA at 37°C, 5% CO_2, overlaid with mineral oil, on culture dishes with coverslip bottom (Mattek). Ten hours after washout from dbcAMP, most oocytes had made their first polar body. Mineral oil and growth medium were drawn off while observing the oocytes with a stereoscope. Freshly made fix (130 mM KCl, 25 mM HEPES pH 6.9, 3 mM $MgCl_2$, 4% paraformaldehyde, 0.15% glutaraldehyde, 0.06% Triton X-100) was gently added to the oocytes and incubated at 37°C for 30 min. Oocytes were permeabilized with PBS + 0.2% Triton X-100 for 10 min at room temperature, blocked in 3% BSA in PBS + 0.1% Tween-20 for 2 hr at room temperature or at 4°C overnight, and stained with anti α-tubulin

(Sigma), phalloidin, and DAPI (included in the mounting medium, Vectashield).

Fixed-Cell Imaging

Samples prepared as above were subjected to imaging within several days of preparation to optimize preservation of fluorescent signal. The 100× objective of an Olympus microscope operated with Softworx software was used to acquire images, which were all identically deconvolved with DeltaVision software (Applied Precision). Z series with 0.2 mm spacing were acquired through the thickness of the sample. Three-dimensional reconstructions were generated using Imaris software (Bitplane).

Supplemental Information

Supplemental Information includes three figures, one table, and two movies and can be found with this article online at doi:10.1016/j.cub.2010.10.030.

Acknowledgments

We thank Karen Oegema, in whose laboratory this work began; Joost Monen and Ed Munro for advice on procedures; Julien Dumont, Julie Canman, and Sara Olson for discussions, reading this manuscript, and sharing unpublished observations; and Jon Audhya and members of the laboratories of Jean-Claude Labbé and Sébastian Carréno for reagents and support. J.F.D. is supported by a postdoctoral fellowship from the Swiss National Science Foundation. A.S.M. receives salary support from the Fonds de recherche en santé du Québec. P.S.M. holds the Canada Research Chair in Chromosome Organization and Mitotic Mechanisms. This work was funded by grants 019162 to A.S.M. and 018450 to P.S.M. from the Terry Fox Foundation and the Canadian Cancer Society Research Institute. A.S.M. dedicates this work to the memory of David W. Borst.

Received: June 5, 2010
Revised: September 6, 2010
Accepted: October 8, 2010
Published online: November 4, 2010

References

1. Deng, M., Suraneni, P., Schultz, R.M., and Li, R. (2007). The Ran GTPase mediates chromatin signaling to control cortical polarity during polar body extrusion in mouse oocytes. Dev. Cell *12*, 301–308.
2. Dumont, J., Million, K., Sunderland, K., Rassinier, P., Lim, H., Leader, B., and Verlhac, M.H. (2007). Formin-2 is required for spindle migration and for the late steps of cytokinesis in mouse oocytes. Dev. Biol. *301*, 254–265.
3. Longo, F.J. (1972). The effects of cytochalasin B on the events of fertilization in the surf clam, Spisula solidissima. I. Polar body formation. J. Exp. Zool. *182*, 321–344.
4. Ma, C., Benink, H.A., Cheng, D., Montplaisir, V., Wang, L., Xi, Y., Zheng, P.P., Bement, W.M., and Liu, X.J. (2006). Cdc42 activation couples spindle positioning to first polar body formation in oocyte maturation. Curr. Biol. *16*, 214–220.
5. Moore, G.D., Ayabe, T., Visconti, P.E., Schultz, R.M., and Kopf, G.S. (1994). Roles of heterotrimeric and monomeric G proteins in sperm-induced activation of mouse eggs. Development *120*, 3313–3323.
6. Zhang, X., Ma, C., Miller, A.L., Katbi, H.A., Bement, W.M., and Liu, X.J. (2008). Polar body emission requires a RhoA contractile ring and Cdc42-mediated membrane protrusion. Dev. Cell *15*, 386–400.
7. Zhong, Z.S., Huo, L.J., Liang, C.G., Chen, D.Y., and Sun, Q.Y. (2005). Small GTPase RhoA is required for ooplasmic segregation and spindle rotation, but not for spindle organization and chromosome separation during mouse oocyte maturation, fertilization, and early cleavage. Mol. Reprod. Dev. *71*, 256–261.
8. Azoury, J., Verlhac, M.H., and Dumont, J. (2009). Actin filaments: Key players in the control of asymmetric divisions in mouse oocytes. Biol. Cell *101*, 69–76.
9. Yang, H.Y., McNally, K., and McNally, F.J. (2003). MEI-1/katanin is required for translocation of the meiosis I spindle to the oocyte cortex in C elegans. Dev. Biol. *260*, 245–259.
10. Piekny, A.J., and Maddox, A.S. (2010). The myriad roles of Anillin during cytokinesis. Semin. Cell Dev. Biol., in press. Published online August 21, 2010. 10.1016/j.semcdb.2010.08.002.
11. Field, C.M., and Alberts, B.M. (1995). Anillin, a contractile ring protein that cycles from the nucleus to the cell cortex. J. Cell Biol. *131*, 165–178.
12. Kinoshita, M., Field, C.M., Coughlin, M.L., Straight, A.F., and Mitchison, T.J. (2002). Self- and actin-templated assembly of mammalian septins. Dev. Cell *3*, 791–802.
13. Straight, A.F., Field, C.M., and Mitchison, T.J. (2005). Anillin binds nonmuscle myosin II and regulates the contractile ring. Mol. Biol. Cell *16*, 193–201.
14. D'Avino, P.P., Takeda, T., Capalbo, L., Zhang, W., Lilley, K.S., Laue, E.D., and Glover, D.M. (2008). Interaction between Anillin and RacGAP50C connects the actomyosin contractile ring with spindle microtubules at the cell division site. J. Cell Sci. *121*, 1151–1158.
15. Gregory, S.L., Ebrahimi, S., Milverton, J., Jones, W.M., Bejsovec, A., and Saint, R. (2008). Cell division requires a direct link between microtubule-bound RacGAP and Anillin in the contractile ring. Curr. Biol. *18*, 25–29.
16. Piekny, A.J., and Glotzer, M. (2008). Anillin is a scaffold protein that links RhoA, actin, and myosin during cytokinesis. Curr. Biol. *18*, 30–36.
17. Sisson, J.C., Field, C., Ventura, R., Royou, A., and Sullivan, W. (2000). Lava lamp, a novel peripheral golgi protein, is required for Drosophila melanogaster cellularization. J. Cell Biol. *151*, 905–918.
18. Field, C.M., Coughlin, M., Doberstein, S., Marty, T., and Sullivan, W. (2005). Characterization of anillin mutants reveals essential roles in septin localization and plasma membrane integrity. Development *132*, 2849–2860.
19. Goldbach, P., Wong, R., Beise, N., Sarpal, R., Trimble, W.S., and Brill, J.A. (2010). Stabilization of the actomyosin ring enables spermatocyte cytokinesis in Drosophila. Mol. Biol. Cell *21*, 1482–1493.
20. Hickson, G.R., and O'Farrell, P.H. (2008). Rho-dependent control of anillin behavior during cytokinesis. J. Cell Biol. *180*, 285–294.
21. Maddox, A.S., Habermann, B., Desai, A., and Oegema, K. (2005). Distinct roles for two C. elegans anillins in the gonad and early embryo. Development *132*, 2837–2848.
22. Zhao, W.M., and Fang, G. (2005). Anillin is a substrate of anaphase-promoting complex/cyclosome (APC/C) that controls spatial contractility of myosin during late cytokinesis. J. Biol. Chem. *280*, 33516–33524.
23. Sönnichsen, B., Koski, L.B., Walsh, A., Marschall, P., Neumann, B., Brehm, M., Alleaume, A.M., Artelt, J., Bettencourt, P., Cassin, E., et al. (2005). Full-genome RNAi profiling of early embryogenesis in Caenorhabditis elegans. Nature *434*, 462–469.
24. Guizetti, J., and Gerlich, D.W. (2010). Cytokinetic abscission in animal cells. Semin. Cell Dev. Biol., in press. Published online August 11, 2010. 10.1016/j.semcdb.2010.08.001.
25. Shimizu, T. (1990). Polar body formation in Tubifex eggs. Ann. N Y Acad. Sci. *582*, 260–272.
26. Oegema, K., Savoian, M.S., Mitchison, T.J., and Field, C.M. (2000). Functional analysis of a human homologue of the Drosophila actin binding protein anillin suggests a role in cytokinesis. J. Cell Biol. *150*, 539–552.
27. Monen, J., Maddox, P.S., Hyndman, F., Oegema, K., and Desai, A. (2005). Differential role of CENP-A in the segregation of holocentric C. elegans chromosomes during meiosis and mitosis. Nat. Cell Biol. *7*, 1248–1255.
28. Munro, E., Nance, J., and Priess, J.R. (2004). Cortical flows powered by asymmetrical contraction transport PAR proteins to establish and maintain anterior-posterior polarity in the early C. elegans embryo. Dev. Cell *7*, 413–424.